Effects of Mesoporous Size and Structure on Solidification Characteristics of Solar Salt

Rui Mao[1,*], *Qirong* Yang[1], and *Zhaoying* Li[1]

[1]Qingdao University, College of Mechanical and Electrical Engineering, 266071, Qingdao, China

Abstract. The effects of mesoporous size and structure on the solidification characteristics of mixed nitrate were simulated by molecular dynamics (MD). The solar salt models of different scales are established by using material Studio software, and the models are exported to the Lammps software package for simulation calculation. The changes of parameters such as radial distribution function, potential energy temperature curve, freezing point, and phase transformation latent heat are summarized, and the micro mechanism of solar salt solidification characteristics at the nanoscale is analyzed. The results show that the freezing point of solar salt increases first and then decreases with the increase of nanopore size, and finally tends to be stable with the increase of nanopore size. The enthalpy of solidification decreases with the increase of scale.

1 Introduction

Phase change materials(PCM) absorb a lot of heat, increase the internal molecular energy at an almost constant temperature, and absorb and release heat in the process of phase change. This characteristic makes it attractive in the medium-temperature thermal energy storage (TES) system of solar thermal utilization and waste heat recovery[1-4]. In recent years, great progress has been made in solar photothermal power generation using molten salt. Solar salt (60wt%NaNO3+40wt%KNO3) is one of the two most popular molten salt media in solar power plants. However, its low thermal conductivity, easy leakage, and undercooling affect the utilization efficiency of solar energy[5-8].

Goitandia et al.[9] analyzed the effects of a eutectic mixture of butyl and fatty acids as PCM confined cycle stability and an undercooling degree from micropores(greater than 0.6nm) to macropores(<200μm). It was found that the nano constraint of silicon increased the undercooling degree by 1-6℃. Kota et al.[10] studied the crystallization behavior of ET in and around two-dimensional mesoporous silica with three different pore sizes(7.5nm, 8.3nm, and 9.2nm). The results show that the phase transition of ET can be controlled by different pore sizes of micro constraints. The above research shows that the pore size of the substrate will affect the thermal properties of CPCM.

In this paper, the MD simulation method is used to explore the effects of mesoporous scale and cooling rate on the solidification characteristics of solar salt. Based on the simulation process of solidification of nano metal particles and microencapsulated phase change materials within the confines, the solar salt models with different ion numbers are established by using Material Studio software. Through the simulation calculation of lammps software package, and potential energy temperature curve, Gibbs free energy, freezing point The micro mechanism of solidification characteristics of solar salt at the nanoscale is analyzed.

2 Simulation

2.1 Model establishment

Build the nitrate molecular model in the Materials Studio software, as shown in Figure 1, and mix $NaNO_3$ and KNO_3 with a mass ratio of 6:4 to build the binary mixed nitrate model. Solar salt models at different scales are established by proportionally increasing or decreasing the number of molecules, as shown in Fig. 2(a)-(f), which are solar salt models with 460, 920, 1380, 1840, 2300, and 2760 molecules in turn. The number of atoms and model scale is shown in Table 1.

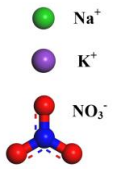

Fig. 1. $NaNO_3$ and KNO_3

Table 1. Molecular numbers of NaNO3 and KNO3 in solar salts(NaNO3:KNO3=6:4)[11]

* Corresponding author: 420698897@qq.com

Molecular number Type	460	920	1380	1840	2300	2760
Na	60	120	180	240	300	360
K	32	64	96	128	160	192
N	92	184	276	368	460	552
O	276	552	828	1104	1380	1656
Model Size	5nm	6nm	7nm	8nm	9nm	10nm

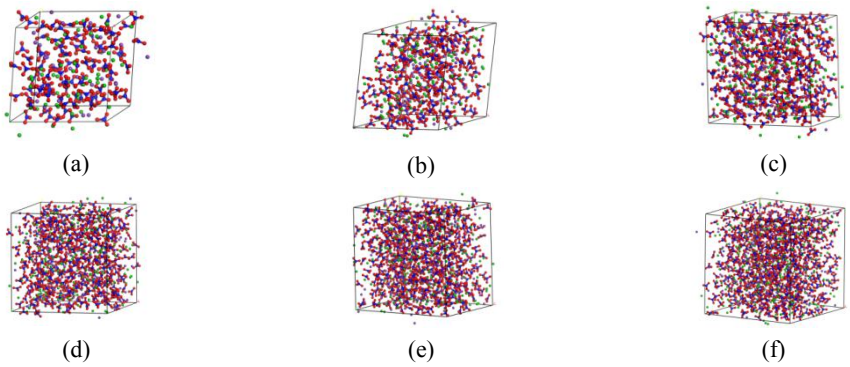

Fig. 2. Solar salt model (a)460; (b)920; (c)1380; (d)1840; (e)2300; (f)2760.

2.2 simulation method

The geometry optimization of the forcite module is used for geometric optimization. The method to evaluate the atomic charge of electrostatic interaction is used current. In the simulation process, atom-based[12] and Ewald[13] methods are used for van der Waals (VDW) and electrostatic interaction (Coulomb) respectively. The temperature is set at 453K-573K, the temperature interval is 10K, and the pressure is set at 0.1GPa. Under the condition of the canonical ensemble (NVT), the method to evaluate the atomic charge of electrostatic interaction is forcefield assigned. PPPM and Ewald are still selected for electrostatic interaction force and van der Waals force, and continue to operate for 70ps to reach equilibrium. Analyze the mean square displacement (MSD) using analysis under the forcite module. The preliminary work of the research group has confirmed the effectiveness of this method[11].

The solar salt model established in MS software is exported to Lammps software package, and the conjugate gradient algorithm is used to minimize the energy. After structural minimization[12], the temperature rises rapidly from 300K to 1000K within 300ps under the NVT ensemble. The electrostatic interaction force is calculated by the PPPM method, and the time step is set to 1fs. L-J and harmonic potential function parameters are shown in Table 2.Using NPT ensemble, the model is first heated and then cooled from 323K to 773K. The simulation parameters are summarized in Table 3. Potential energy, kinetic energy, enthalpy, and total energy are obtained.

Table 2 Potential parameters of Solor Salt composites[14-15]

Atom	Q[e]	E[eV]	σ[Å]
Na	1	6.6373×10^{-3}	2.407
K	1	4.336×10^{-3}	3.188
N	0.95	4.017509×10^{-3}	3.431
O	-0.65	3.469129×10^{-3}	3.285

Table 3 Simulation parameters

Number of Atoms	460、920、1380、1840、2300、2760
Timestep (fs)	1
Pressure (Pa)	1×10^{5}
Ensemble	NPT
Cooling Rates (K/ps)	0.1

In this simulation, the density of solar salt is 1.802g/cm3, the simulated value of Wu Chenguang et al.[15] is 1.73g/cm3, with an error of 4.16%, and the experimental value of Nicole et al.[16] is 1.79g/cm3, with an error of 0.67%. The error is less than 5%, which can verify the accuracy of the simulation.

$$\overline{E_k} = \frac{1}{2}(n+1)\overline{U} \quad (1)$$

The results of molecular dynamics simulation depend on the selected potential function.According to virial theorem (equation 1), the average kinetic energy and

average potential energy of the system are linearly related:

Through equilibrium molecular dynamics simulation, the self-diffusion coefficient D (m2/s) can be calculated by the Einstein method. Einstein relation[17] can be expressed as:

$$D = \lim_{t\to\infty} \frac{1}{6Nt} \sum_{i=1}^{N} \langle [r_i(t) - r_i(0)]^2 \rangle \quad (2)$$

$$\frac{G}{R_g T} - \left(\frac{G}{R_g T}\right)_{ref} = \int_{T_{ref}}^{T} -\frac{H}{R_g T^2} dT \quad (3)$$

3 Results & Discussion

3.1 Potential energy

Taking the solar salt containing 460 molecules as an example, the potential energy function of particles during heating and cooling is shown in Fig. 3(a). For pure materials, whether melting or solidification, the potential energy jumps obviously at a certain temperature, which is the phase transition temperature, and the potential energy changes linearly with the temperature before and after this jump.

The potential energy temperature curves of solar salt nanoparticles with different sizes at the cooling rate of 0.1K/ps are drawn as shown in Fig. 3(b). The potential energy of solar salt nanoparticles with different sizes has the same variation law with temperature, and there is a potential energy step between 448K-548K. At the same simulated temperature, the potential energy increases with the increase of solar salt scale, and the phase transition latent heat increases with the increase of solar salt scale. The simulated latent heat of phase transition at 2760 molecular numbers is about 117kJ/kg, which is within a reasonable error range from the experimental value of 116kJ/kg in reference[18].

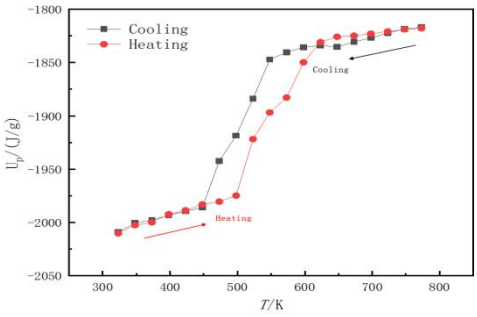

(a)

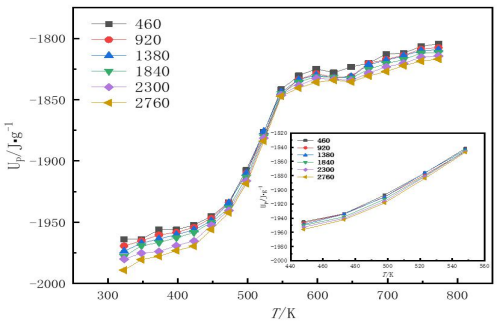

(b)

Fig. 3 Potential energy temperature curve (a) 460 molecular number rise and drop temperature curve; (b) Cooling curves of nanoparticles with different scales.

3.2 Freezing point

The faster the diffusion in the binary nitrate system, the stronger the fluidity of ions in the system. Therefore, when the value of the self-diffusion coefficient changes significantly, it indicates that phase transition occurs at this temperature.

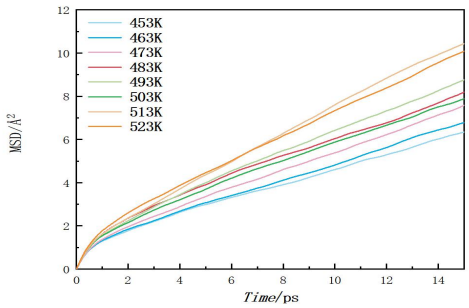

(a)

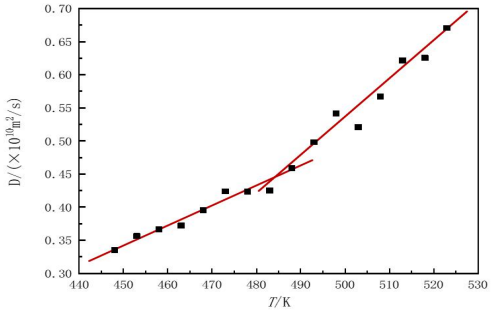

(b)

Fig. 4. Mean square displacement and self diffusion coefficient of solar salt with ion number 2760: (a) mean square displacemen; (b)self diffusion coefficient.

The mean square displacement and self-diffusion coefficient of solar salt with 2760 ions in nanopores at different temperatures are shown in Fig. 4. The freezing point of solar salt at different scales is calculated. Our research group has calculated the melting point of nanoparticle solar salt at different scales, and the simulation results are summarized in Table 4. The simulation results show that the melting point and freezing point of solar salt are different at the same scale, and the melting point of particles is greater than the freezing point. This shows that the liquid-solid transition lags behind the solid-liquid transition at the nanoscale, which has been confirmed in theory and experiment[19], and also proves that it is more difficult to change from disorder (liquid) to order (solid) than from order to disorder.

$$\frac{T_c(r_{np})}{T_c(\infty)} = 1 - \frac{4V_s\gamma_{sl}r_{np}H_c(T)}{1-\frac{\delta}{r_{np}}} \qquad (r_{np} < 10nm) \qquad (4)$$

Where, $T_c(r_{np})$ is the solidification temperature of nanocrystals, r_{np} is the radius of nanoparticles, $T_c(\infty)$ is the solidification temperature of blocks, V_s is the molar volume of bulk crystals, γ_{sl} is the interface energy of solid-liquid phase, $H_c(T)$ is the molar solidification enthalpy, and δ is the thickness of a liquid layer at the surface.

For the liquid-solid phase transformation with uniform nucleation, the change with temperature is very small. According to formula (4), when the diameter of nanocrystals is less than 10 nm, it is equivalent to the scale, and the specific surface area has a great influence on the phase transition temperature. Since the specific surface area (surface area/mass) of solar salt is inversely proportional to the diameter, within a certain scale range, the specific surface area will increase significantly with the decrease of the number of ions. At this time, the nucleation is unstable and the formed crystal nucleus is easy to disappear. It is necessary to form a stable crystal nucleus when it is cooled to the freezing point under the condition of large undercooling.

It can be seen from table 4 that with the increase of the number of ions, the melting point increases first and then decreases, reflecting the scale effect of nitrate solidification characteristics at the nano scale.

Table 4. Phase transition temperature of solar salts at different scales

Molecular number	460	920	1380	1840	2300	2760	5520
Melting point/K	493	493	503	518	508	493	493
Freezing point/K	463	483	473	503	490	483	478

460 molecular number solar salt has a freezing point of 463K and a melting point of 493K.The reason for this phenomenon is that the proportion of surface energy of surface atoms in the total energy of particles changes.

3.3 Latent heat of phase change

The difference of system energy before and after solidification is solidification enthalpy (latent heat of solidification phase transformation). The latent heat of phase change represented by the corresponding potential energy difference of the system in Section 3.1 is summarized in Table 5. The simulation results show that the potential energy of solar salt system decreases with the decrease of temperature, and the solidification enthalpy decreases with the increase of scale.

Table 5. Phase transition latent heat of solar salts at different scales

Molecular number	460	920	1380	1840	2300	2760
Latent heat/(kJ/kg)	108.75	109.39	110.12	112.25	114.69	117.57

Similar to bulk materials, the solidification enthalpy of nanomaterials can also be expressed as the product of solidification entropy and freezing point, so formula (5) can be obtained.

$$\frac{H_c(r_{np})}{T_c(r_{np})} - \frac{H_c(\infty)}{T_c(\infty)} = \left(\frac{3k_B}{2}\right)\ln\left[1 - \frac{5r_0}{\frac{1}{\mu^2}r_{np}}\right] \qquad (5)$$

Where, ∞ represents block; r_0 is the atomic radius, nm; r_{np} is the radius of nanoparticles, nm; μ is the shape factor, the value of spherical particles is 1, H_c is the molar enthalpy of solidification, J/mol; S_c is solidification entropy, J/(mol·K); k_B is Boltzmann constant, 1.38×10^{-23}J/K.

It can be seen that when the particle size increases, the solidification enthalpy of nanoparticles increases, and when $r_{np}\to\infty$,the solidification enthalpy tends to be close to the block solidification enthalpy. Since the solidification point increases first and then decreases with the increase of scale, it is obtained from formula (5) that the solidification enthalpy increases faster with the increase of scale, which is consistent with the results obtained by simulation and the law obtained by Eryürek[20] et al.

4 Conclusions

Because it is difficult to observe the solidification process of phase change materials with nanopore size in the experiment, the solidification characteristics of solar salts with different scales are studied by equilibrium molecular dynamics simulation. The conclusions are as follows:

1) With the increase of ion number, the melting point of solar salt increases first and then decreases, indicating that the pore size of the skeleton has an optimal value.

2) The potential energy of the solar salt system decreases with the decrease of temperature, and the solidification enthalpy decreases with the increase of scale.

References

1. Z. Jiang, G. Leng, F. Ye, Z. Ge, C. Liu, L. Wang. Energy Conversion & Management, **106**(DEC.), 165-172 (2015)
2. E. Alehosseini, S. Jafari. M. Trends in Food Science & Technology, **91**, 116-128 (2019)
3. M. Umair, Y. Zhang, S. Zhang, B. Tang. Applied Energy, 235 (2019)
4. X. Chen, H. Gao, M. Yang, L. Xing, W. Dong, A. Li. Energy Storage Materials, **18**, 349-355 (2019)
5. Y. Feng, D. Feng, X. Zhang Phase transition And Heat transport properties of mesoporous composites (Beijing: Science Press) pp110-113 (in Chinese) (2019)
6. X. Chen, Z. Tang, Y. Chang, H. Gao, J. Lv. iScience **23(10)**, 101606 (2020)
7. T. Qian, J. Li, M. Xin, B. Fan. Acs Sustainable Chemistry & Engineering, **6(1)** (2017)
8. C. Xiao, A. Hg, A. Lx, A. Wd, A. Al, B. Pc. Energy Storage Materials, **18**, 280-288 (2019)
9. A. M. Goitandia, G. Beobide, E. Aranzabe, A Aranzabe. Solar Energy Materials & Solar Cells, **134**, 318-328 (2015)
10. K. Nakano, Y. Masuda, H. Daiguji. Journal of Physical Chemistry C, **119(9)**, 150205115437003 (2015)
11. Z. Y. He, Q. R. Yang, Z. Y. Li, R. Mao, L. W. Wang, C.X.J. Yan, /OL Acta Phys. Sin 1-23
12. N. Karasawa, W. Goddard Macromolecules (1992).
13. G. Pan, J. Ding, W. Wang, International Journal of Heat and Mass Transfer **103** 417 (2016)
14. G. Hu, B. Cao. Journal of Applied Physics, **114(22),** 96 (2013)
15. C. Wu, B. Li. J/OL Journal of composites: 1-11
16. P. Nicole, B. Thomas, M. Claudia, E. Markus, W. Antje. Beilstein Journal of Nanotechnology, **6(1)**, 1487-1497 (2015)
17. D. Sheppard, R. Terrell, G. Henkelman. Journal of Chemical Physics, **128(13)**, 385-404 (2008)
18. M. K. Saranprabhu, K. S. Rajan. Renewable energy, **141**(OCT.), 451-459 (2019).
19. K. Pan, Y. Li, Q. Zhao, S. Zhang. JOM (2018)
20. M. Eryürek, Güven. Physica A: Statistical Mechanics and its Applications, **377(2)**, 514-522 (2007)